EMAS
Engineering Modelling, Analysis & Simulation
THE NAFEMS JOURNAL

NAFEMS
Vol. 3, Issue 1, 2026

Thermo-Mechanical Degradation of EPDM Seals in EV Inverter Environments: A Study of Mullins Effect and Viscoelastic Relaxation

Bharath P T[a], Vipin Das[a], Ted Zeunik[b]

[a]BorgWarner India Propulsion Engineering Centre, Bangalore, India, 560067
[b]BorgWarner Technical Centre, Kokomo, United States of America, 46902

Abstract

Electric Vehicle (EV) inverters are essential components in the powertrain of electric vehicles, converting direct current (DC) from the battery into alternating current (AC) to power the electric motor. The seals within EV inverters are critical for maintaining system integrity, preventing contamination, and ensuring the proper functioning of inverter components. This study focuses on the performance of High Voltage Direct Current (HVDC) Press-In-Place (PIP) seals made from Ethylene Propylene Diene Monomer (EPDM) rubber, a Hyperelastic material known for its large elastic deformation and incompressibility.

The research investigates the mechanical performance of EPDM PIP seals for three material conditions: Least Material Condition (LMC), Nominal Material Condition (NMC) & Maximum Material Condition (MMC). The EPDM PIP seals were evaluated at different temperatures up to 1000hrs and under Thermal Cyclic loading.

A combined simulation approach incorporating the Mullins effect and viscoelastic relaxation was adapted to model stress softening over multiple thermal cycles and up to a large duration of 1000hrs. Results indicate that the PIP (Press-in-place) seals lose contact pressure during thermal cycling due to Stress Relaxation & Mullin's effect occurring due to expansion & contraction of seals inducing cyclic Thermal strains. The results also reveal significant stress-softening in early cycles due to change in polymer chain structure, followed by gradual stabilization. Viscoelastic effects contribute to stress decay during hold periods, impacting long-term sealing performance. The study provides insights into the interplay between material behaviour and thermal loading offering design direction for improving seal reliability in EV inverter systems.

Keywords

EPDM, Plane Strain, Prony series, Mullin's Effect, Stress relaxation, PIP seals, EV Inverters, FEA.

1 Introduction

This study centres on the simulation of seals used within EV inverters, typically made from rubber materials like EPDM and commonly shaped as O-rings. A major concern with rubber components is their susceptibility to creep—gradual deformation over time—which can lead to a permanent set. This permanent deformation reduces the compressive force on the seal, potentially compromising its ability to maintain a proper seal. In EV inverter environments, elevated temperatures exacerbate this issue by accelerating the degradation of rubber materials. To address these challenges, finite element (FE) modelling is employed to simulate seal behaviour. FE modelling is particularly effective for analysing

[1]Corresponding author.
E-mail address: bharathp@borgwarner.com (Bharath P T)
https://doi.org/10.59972/1fmysqjp

complex geometries and material responses, although the non-linear and time-dependent nature of rubber adds significant complexity to the simulations.

1.1 Hyperelasticity and Stress Relaxation

In joints, rubber deforms significantly compared to surrounding materials such as Aluminium, maintaining sealing pressure even when components shift [1]. This behaviour is modelled using Hyperelasticity—a generalization of Hooke's law suitable for large strains. Rubber also shows time-dependent behaviours like creep and permanent set. Hyperelastic models are based on energy density potentials, which ensure reversible deformation. Several models exist, including Neo-Hookean, Mooney-Rivlin, Arruda-Boyce, Ogden, and Yeoh. For typical compressive strains in O-rings (e.g., upto 120% engineering strain), the Neo-Hookean model is sufficient, while more advanced models are needed for large tensile strains where polymer chains are heavily stretched.

The Neo-Hookean energy potential is the simplest and is:

$$\Phi = C_{10}\left(J^{-2/3}I_1 - 3\right) + \frac{1}{D_1}(J-1)^2 \tag{1}$$

where $I1 = \lambda_{12} + \lambda_{22} + \lambda_{32}$ is the first invariant, $J = \lambda_1\lambda_2\lambda_3$ is the volume ratio and λ_i are principal stretches. Like the linear elastic model, it has only two material parameters: C_{10} and D_1 that governs elasticity similarly as Young's modulus E and the bulk modulus respectively in linear elasticity. In linear elasticity one often defines the behaviour with the parameter Poisson's ratio ν which relates to the compressibility. For the Neo-Hookean model the relations are:

$$C_{10} = \frac{E}{4(1+\nu)}, \quad D_1 = \frac{6(1-2\nu)}{E} \tag{2}$$

The viscoelastic behaviour of a material can be represented by combining a Hyperelastic model with a suitable mathematical model to add the effect of time, which is the Prony series model used in this study.

$$\sigma_{\text{total}} = \sigma_{\text{Hyperelastic}} + \sigma_{\text{viscoelastic}} \tag{3}$$

The mathematical model for stress relaxation is given by:

$$\alpha_i = \frac{G_i}{G_0} \tag{4}$$

$$G(t) = G_0\left[\alpha_\infty^G + \sum_{\{i=1\}}^{\{N\}} \alpha_i^G e^{\left\{\{t\}/\{\tau_i^G\}\right\}}\right] \tag{5}$$

where α_i is the relative moduli which is the ratio of the Prony component G_i and initial shear moduli G_0 and G_∞ is the long-term shear moduli at time t=∞, G(t) is the relaxation/shear moduli at time t and τ_i is the relaxation time of the Prony component Gi, α_i and τ_i can be obtained by choosing the number of Prony series 'i' terms and fitting the equation to the data from the relaxation test. The curve fitting algorithm available in FEA tool can be used to obtain the Prony coefficients.

1.2 Mullin's Effect

The Mullin's effect [9] is characterized by a reduction in material stiffness during loading, which becomes evident in cyclic loading where the unloading path differs significantly from the loading path. Mullin's material models treat the virgin material using standard Hyperelastic potentials and incorporate Mullin's effect adjustments based on the maximum load experienced in the material's history.

In the diagram displayed in Figure 1. the material is first stretched to point (1) followed by the initial loading path. After point (1) the material is unloaded to the unstretched state and then reloaded to point (1) again. The stress-stretch ratio curves are shown in the figure, and the Mullins effect is clearly seen. The material is then further stretched past point (1) to point (2). No Mullins effect occurs after point (1).

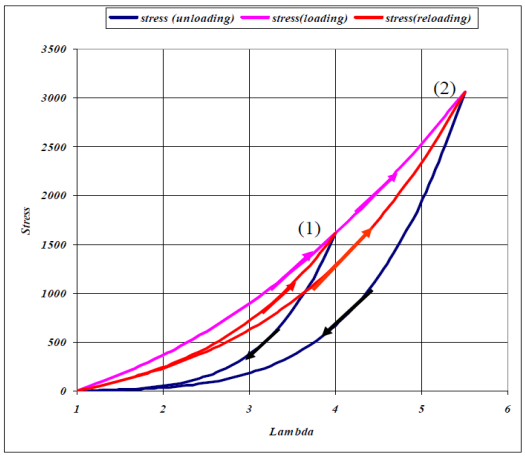

Figure 1. Mullin's Effect for uniaxial loading, unloading and subsequent reloading [8].

2 Materials and Methods

Figure 2. shows the project overview starting with field failure observed during leak test followed by Root Cause analysis using Ishikawa Diagram in Figure 3.

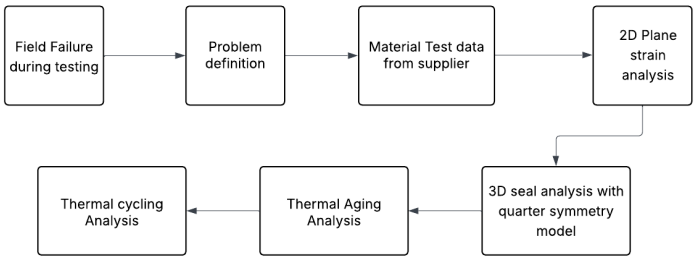

Figure 2. Project Overview.

As shown in Figure 3, Root Cause Analysis was carried out and found that Housing Fixture Machining was exceeding the allowable design specs leading to Seal Compression below LMC target. The material testing was carried by the seal supplier and after material characterisation and further preliminary studies the material constants were obtained for the sealing simulations.

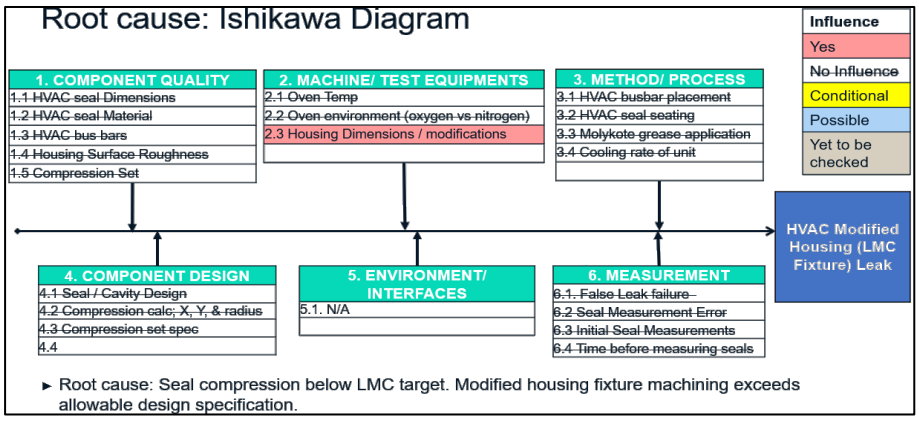

Figure 3. Ishikawa Diagram.

2.1 Seal Assembly procedure

- Seal Installation Process: Lubricant is applied to the seal before placing it on the HVAC plastic header Figures 4 and 5, which is then inserted into the housing cavity until bolting surfaces align and are fastened.

- Gap Measurement (A): LMC, NMC, MMC are manufacturing tolerances affecting the interference fit between the seal and groove and based on those material & manufacturing tolerances the values of gap would differ. The gap between the housing screw boss and header mounting surface is 2.49 mm for LMC, 3.9 mm for NMC and 4.9 mm for MMC and affecting seal behaviour during assembly.
- Seal Rolling Risk: A larger initial gap (Δs) between the seal and busbar edge, combined with high friction, increases the likelihood of seal rolling during busbar insertion. To minimize seal rolling and ensure smooth insertion, Δs should be minimized and friction reduced—optimal coefficient of friction found to be 0.1 through study.
- Friction Impact: Higher friction between the seal and housing raises the risk of gap extrusion and improper seal placement.
- Limiting factors: Seal Contact pressure should not go below 1 MPa and maximum equivalent strain should not exceed 255%.

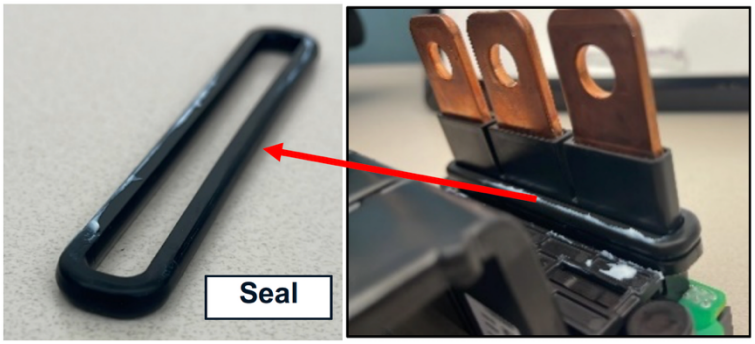

Figure 4. HVAC Busbar assembly.

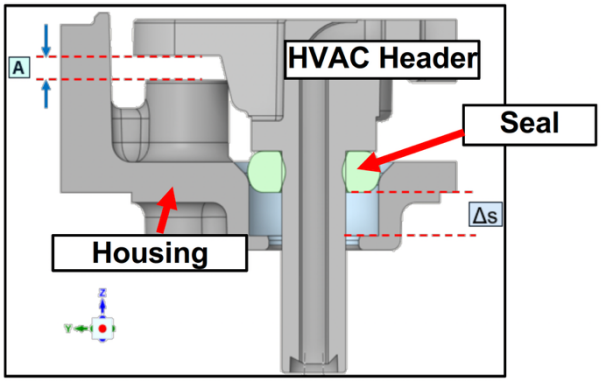

Figure 5. Seal Assembly section view.

2.2 Materials

In Figure 5, the HVAC seal assembly consists of Inverter housing, HVAC Header and PIP (Press in Place) seal. As mentioned in Table 1. the Housing and HVAC Header are Aluminium EN AC-43500 and PBT-GF30 material respectively and Isotropic Elastic material model is used. HVAC Seal is of EPDM material and modelled using Temperature dependant Hyperelastic and Viscoelastic material models.

Table 1. Linear isotropic material properties.

Part	Material	Density (kg/m^3)	Young's Modulus (MPa)	Poisson's Ratio	CTE (10^{-6})/°C)
HVAC Header	PBT-GF30	1500	10 500	0.35	22
Housing	EN AC-43500 Aluminium	2700	71 000	0.3	25

2.2.1 Material modelling, Hyperelastic and Viscoelastic

The dominant deformation mode of the seal within the assembly can be identified through analysis of the invariants of the Cauchy-Green deformation tensor and indicates that the gasket primarily undergoes pure shear deformation, while uniaxial and Equi-biaxial tension are not observed in this application. The final material model selection for the seal is based on the analysis of residuals and seal strain behaviour. As shown in Table 2, the material stiffness is modelled using the incompressible Neo-Hookean model, which is defined by a temperature single material constant obtained after the material characterisation by the seal supplier and with constant coefficient of thermal expansion (CTE). This constant can also be derived from the nominal Shore A hardness of the EPDM rubber using the empirical relation proposed by Battermann & Koehler [12].

$$C_1 = 0.086 \times 1.045^{\mathrm{ShA}} \tag{6}$$

Table 2. Temperature dependent shear moduli for EPDM Seal with CTE.

Temperature (°C)	Initial Shear Modulus Mu (MPa)	CTE (10-6)/°C)
-40	2.3	200
22	1.2	200
150	0.89	200

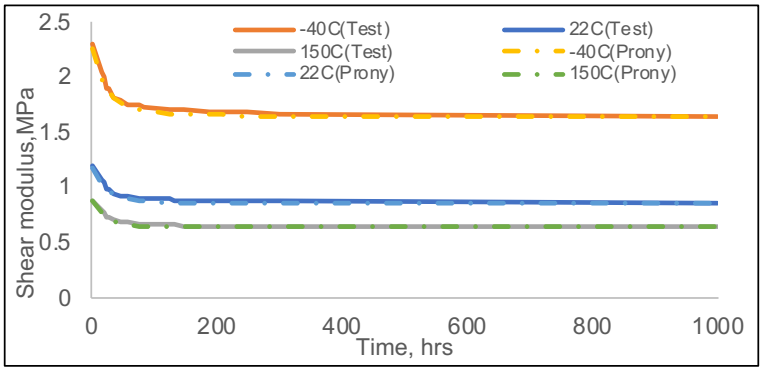

Figure 6. Viscoelastic curve fitting (at different temperatures).

In Figure 6, the Stress Relaxation curves obtained for three different temperatures are curve fitted using Viscoelastic Prony Series model with 3 parameters which provides the Relative Moduli and Time constants for each index.

2.2.2 Material Modelling: Mulin's Effect

The pseudo-elastic model of the Mullins effect is a modification of the standard thermodynamic formulation for Hyperelastic materials and is given by:

$$W(F_{ij,n}) = \eta\, W_0(F_{ij}) + \phi(\eta), \tag{7}$$

where W_0(Fij) is the base strain energy function, typically representing the undamaged or reference material behaviour, W(Fij,n) is the total strain energy density, η is an evolving scalar damage variable and ϕ(η)= Damage function.

The modified Ogden-Roxburgh damage function has the following functional form of the damage variable:

$$\eta = 1 - \frac{1}{r}\, erf\left(\frac{W_m - W_0}{m + \beta W_m}\right) \tag{8}$$

where r, m, and β are material parameters and W_m is the maximum virgin potential:

$$W_m = \max!\,[W_0(t)] \text{ over the time interval } t \in [0,\, t_0] \tag{9}$$

Based on the cyclic loading-unloading test curves obtained for different strains, r, m, and β values were obtained by curve fitting for different temperatures where [9]:

- r: Damage parameter controlling the magnitude of softening, range: 0.1<r<1 and Higher r → more softening.

- m: Controls the rate of damage evolution, range: 0.1<m<10 and larger m → slower transition from virgin to damaged state.
- β (sometimes introduced in extended models): Scales the energy term or modifies the exponential decay, range: 0.1<m<5 and influences how quickly the material approaches the softened state.

2.3 FEA Model

A 3D Quarter Symmetrical Model, displayed in Figure 7.a. of the HVAC seal assembly is used for FEA analysis and is meshed in the Ansys Mechanical using Hex dominant method (meshing statistics in Table 3.) with sufficient refinement to capture accurate contact pressures and seal strains.

Table 3. Meshing Information (3D Quarter Symmetrical Model).

Part	Element type	Total Element count	Total Node count
Housing		32359	29795
HVAC Header	Hex 8	20187	18453
Seal		43200	47464

Figure 7.b. shows that displacement is applied on the face (highlighted in yellow). In the FEA model the housing (highlighted in green) is fixed in all degrees of freedom throughout the simulation steps.

A Plane Strain Model (2D) (Figure 8.a.) of the HVAC seal assembly which is used for FEA analysis. The assembly is meshed in the Ansys Mechanical using Quadrilateral dominant method (Table 4) with sufficient refinement to capture accurate contact pressures and seal strains.

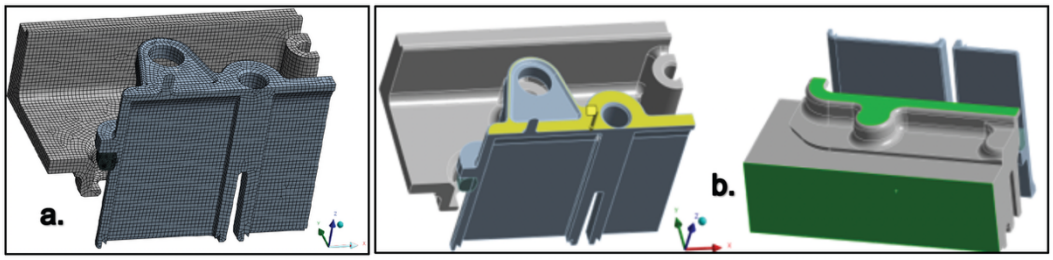

Figure 7. a. Quarter symmetrical FE model, b. Displacement & Fixed Boundary conditions.

Table 4. Meshing Information (2D Plane Strain Model).

Part	Element type	Total Element count	Total Node count
Housing		3319	3515
HVAC Header	Quad 4	378	439
Seal		269	299

The contacts at Housing-Seal and Header-Seal interfaces are modelled using nonlinear frictional contacts with 0.1 friction coefficient and with Augmented Lagrange formulation.

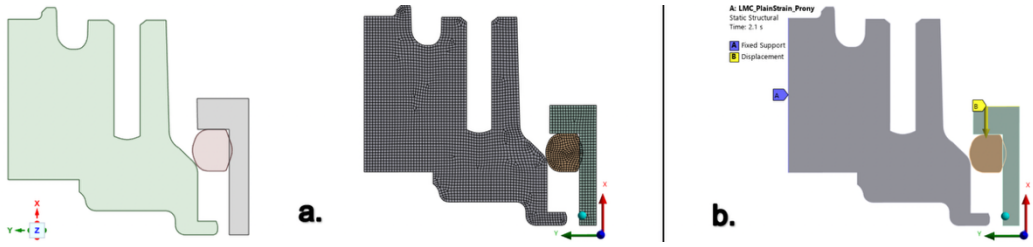

Figure 8. a. 2D Plane Strain FE model, b. Displacement & Fixed Boundary conditions.

2.3.1 Simulation setup for Thermal ageing

- Model Setup: Quarter symmetrical model with respective CTE values; initial interference resolved in CAD.
- Assembly Step: HVAC plastic overmold with seal displaced into aluminium housing until screw boss contact.

- Thermal Load: Thermal ageing performed for cooling 22°C to -40°C & Heating from 22°C to 150°C.
- Material Behaviour: Stress relaxation effect considered to simulate long-term seal deformation.

2.3.2 Simulation setup for combined Thermal ageing and Thermal cycling

- Similar Model Setup and Assembly Step as Thermal Ageing followed by below steps:
- Thermal Load: Cyclic temperature variation from 22°C → -40°C → 95°C for 3 cycles (Figure 9).
- Material Behaviour: Mullin's effect and stress relaxation modelled to capture cyclic strain softening and recovery.

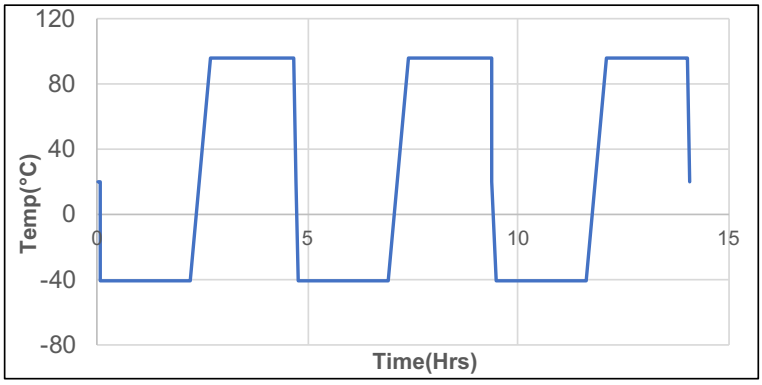

Figure 9.Thermal Cycling Profile.

3 Results and Discussion

The study was conducted initially using 2D plane strain models with Stress Relaxation effects to understand the behaviour of the seal at various temperature conditions. However, due to the limitation of the 2D plane strain model not able to capture various outputs such as contact pressure, max equivalent strain at different sections of the seal. A 3D Quarter Symmetry model is considered for simulation which closely resembles the seal behaviour during an actual physical test. The seal was simulated without directly constraining any point on the seal to capture the contact pressure completely throughout the seal surface. Since this is a highly nonlinear problem and can cause convergence issues while solving using traditional implicit solver, semi-implicit method [11] was used.

The study shows the effect of Stress Relaxation and Mullins effect on Seal Deformation, Contact Pressure and Maximum Equivalent Strain for various material conditions and thermal loading cases.

- 2D Plane Strain model (with Stress relaxation and temperature-dependent property)
- 3D Quarter Symmetry model (without Stress relaxation and temperature-dependent property)
- 3D Quarter Symmetry model (with Stress relaxation and temperature-dependent property)
- 3D Quarter Symmetry model (with Stress relaxation and temperature-dependent property with Mullin's effect)

3.1 Thermal Ageing

3.1.1 With Stress Relaxation effects (2D Plane Strain Results)

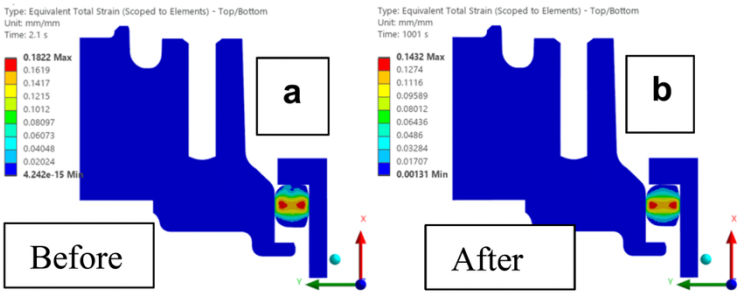

Figure 10. LMC (-40°C) Total Strain.

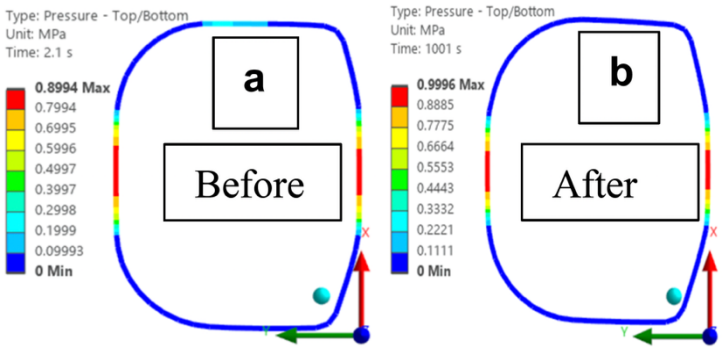

Figure 11. LMC (-40°C) Contact Pressure.

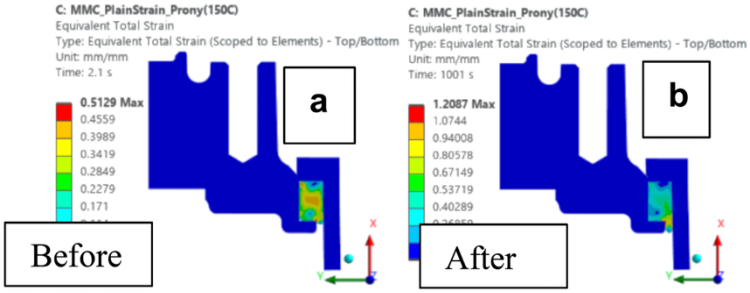

Figure 12. MMC (150°C) Total Strain.

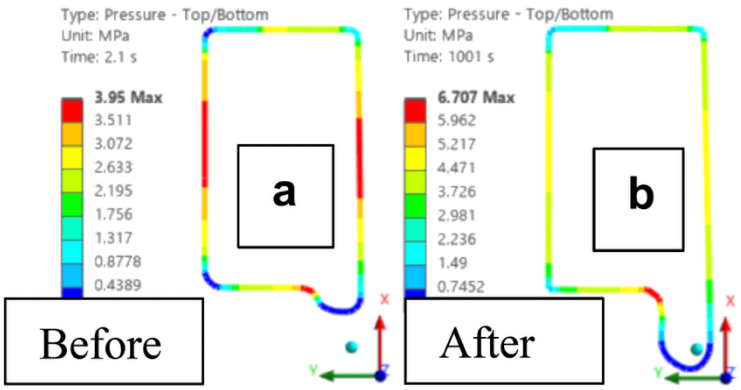

Figure 13. MMC (150°C) Contact Pressure.

Figure 11.a. displays LMC at -40°C, Contact Pressure of 0.89MPa at time 2hrs & 0.99MPa at time 1000 hrs. There is a reduction on Max Seal Deformation and Equivalent Strain/Total Strain due to shrinking of seal while cooling to -40°C and Contact Pressure has increased at the end of 1000hrs during the Stress Relaxation step as the Contact Pressure lost during shrinkage of Seal is partially compensated

when the material adjusts and settles into a more stable state after 1000hrs. The Max Strain observed for the MMC conditions are at 150°C is 121% after 1000hrs. Max Deformation observed is 6.7mm for 150°C after 1000hrs. Contact Pressure is maintained above 1MPa for MMC condition.

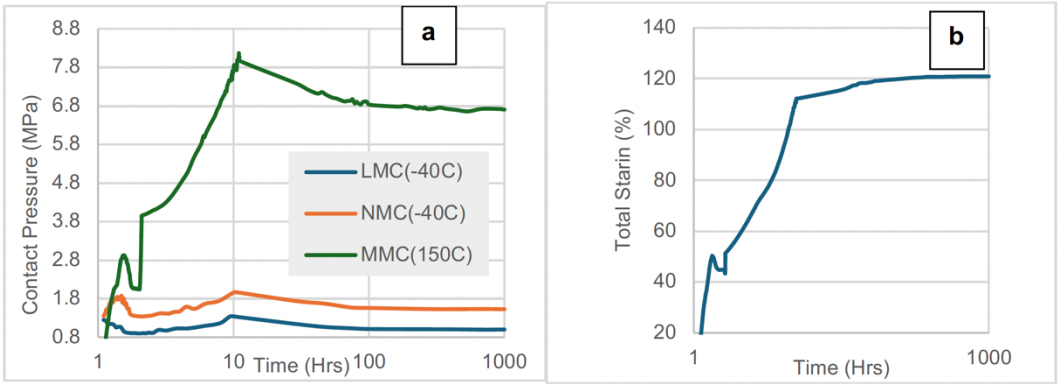

Figure 14. 2D Seal: a. Contact Pressure, b. MMC Total Strain (at 150°C).

In Table 5., the seal contact pressure is below 1MPa for all the LMC cases whereas it is above 1MPa for the MMC cases. Highest maximum equivalent strain is observed at 150°C for both the LMC and MMC cases. With time, the contact pressure decreases, and maximum equivalent strain increases due to stress relaxation.

Table 5. 2D Plane Strain results with Stress Relaxation.

LMC					MMC				
Temperature (C)	Time (Hrs)	Max Deformation (mm)	Max Equivalent Strain (%)	Max Contact Pressure (MPa)	Temperature (C)	Time (Hrs)	Max Deformation (mm)	Max Equivalent Strain (%)	Max Contact Pressure (MPa)
22	2.1	2.75	18.22	0.8994	22	2.1	6.21	47	4
	1001.1	2.76	18.23	0.6516		1001.1	6.26	53	3.3
-40	2.1	2.7499	18.22	0.8994	-40	2.1	5.9	51	4.4
	1001.1	2.673	14.32	0.9996		1001.1	6.2	40	3.2
150	2.1	2.7475	18.21	0.8994	150	2.1	6.2	51	3.95
	1001.1	3.0846	25.46	0.6577		1001.1	7.4	121	6.7

3.1.2 Without Stress Relaxation effects (3D Quarter Symmetry Results)

In Figure 15.b., the Contact Pressure is below the minimum Contact Pressure criteria of 1 MPa between casting and Seal at corner and at the end of Seal Compression at 22°C and at -40°C step (Figure16. b.) hence would not be leak proof.

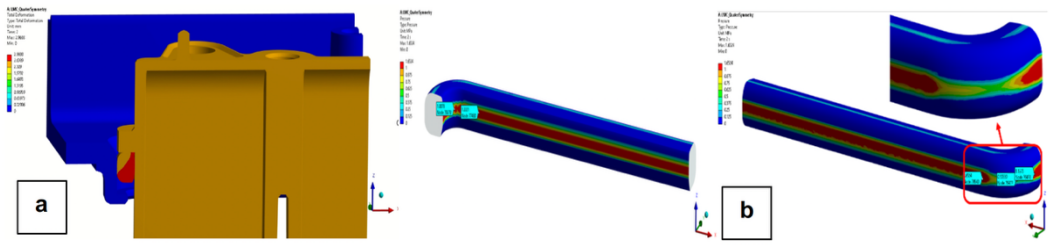

Figure 15. LMC (22°C): a. Total Deformation, b. Contact Pressure of Seal.

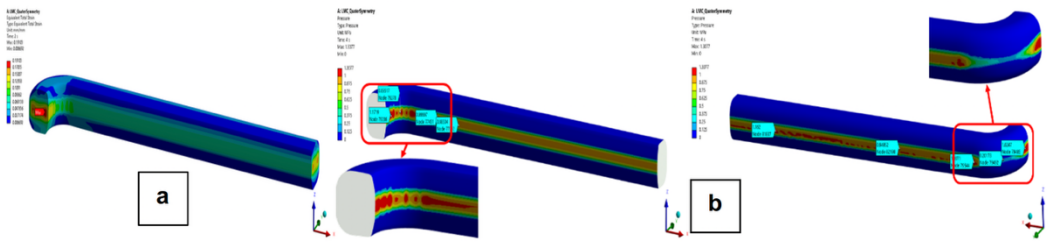

Figure 16. LMC (22°C) a. Total Strain, b. LMC (-40°C) Contact Pressure.

In Figure 17.a. the Minimum Contact Pressure of 1 MPa is maintained on the contact surfaces and seal interfaces are in sticking condition at the end of the seal compression for NMC cases at -40°C, hence would be leak proof. [Figure 17.b.] Maximum Equivalent Strain observed in NMC (Nominal material condition) is well below the failure limits of 255% for PIP (Press in place) seal at -40°C.

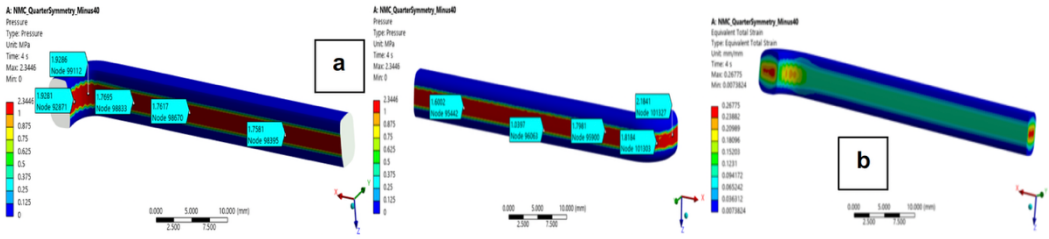

Figure 17. NMC (-40°C): a. Contact Pressure, b. Total Strain.

Table 6. Without Consideration of Stress Relaxation or Mullin's Effect.

LMC				NMC				MMC			
Temperature (°C)	Max Deformation	Max Equivalent	Max Contact Pressure	Temperature (°C)	Max Deformation	Max Equivalent	Max Contact Pressure	Temperature (°C)	Max Deformation	Max Equivalent	Max Contact Pressure
	(mm)	Strain (%)	(MPa)		(mm)	Strain (%)	(MPa)		(mm)	Strain (%)	(MPa)
22	2.96	19.1	1.65	22	4.62	30.15	2.71	22	5.82	48.77	5.84
-40	2.96	17.98	1.3	-40	4.62	26.67	2.34	-40	5.88	45.46	3.91
150	3.2	23.66	1.94	150	5.01	37.61	3.16	150	6.73	97.04	8

3.1.3 With Stress Relaxation effects (3D Quarter Symmetry Results)

In Figure 18.b the Contact Pressure is below the minimum Contact Pressure criteria of 1 MPa at corners & other areas of contact interfaces at the end of Seal Compression for -40°C step, which is attributed to shrinking of Seal due to Cooling and Stress Relaxation effect causing a notable difference in Contact Pressure change in comparison to model without Stress Relaxation effect, hence would not be leak proof. For other two cases, the minimum contact pressure are above 1 MPa limit. Max strain of 46% is observed for MMC 150°C case.

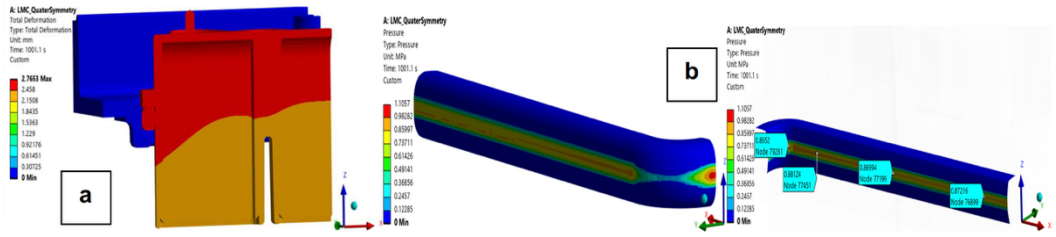

Figure 18. LMC (-40°C): a. Total Deformation, b. Contact Pressure of Seal.

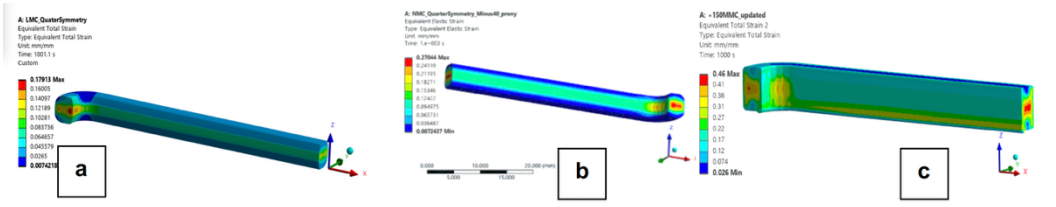

Figure 19. a. LMC (-40°C), b. NMC (-40°C) c. MMC (150°C) Total Strain.

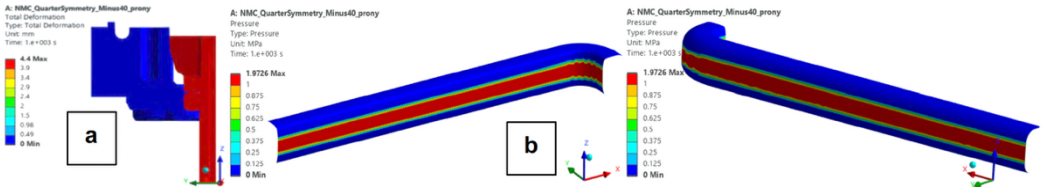

Figure 20. NMC (-40°C): a. Total Deformation, b. Contact Pressure of Seal.

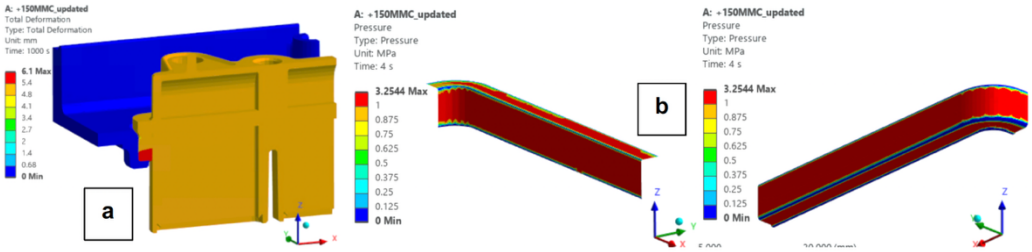

Figure 21. MMC (150°C): a. Total Deformation, b. Contact Pressure of Seal.

Table 7. Thermal ageing.

Cases	Max Deformation (mm)	Max Equivalent Strain (%)	Max Contact Pressure (MPa)
LMC @ -40˚C	2.76	18	1.1
NMC @ -40˚C	4.4	27	1.97
MMC @ 150˚C	6	46	3.25

Figure 22 and Figure 23 show the cooling/heating step followed by maintaining the loads (both compression and thermal) on seal assembly up to 1000hrs. It can be observed in all cases that the contact pressure rises then decreases gradually and becomes constant. The total strains increase during the thermal step and then remains constant.

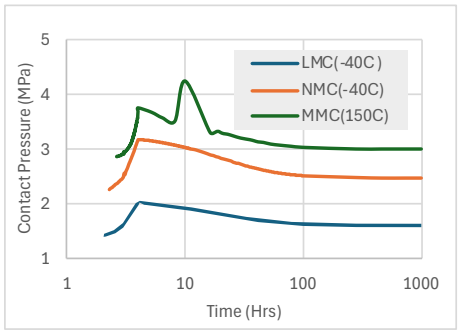

Figure 22. Contact pressure.

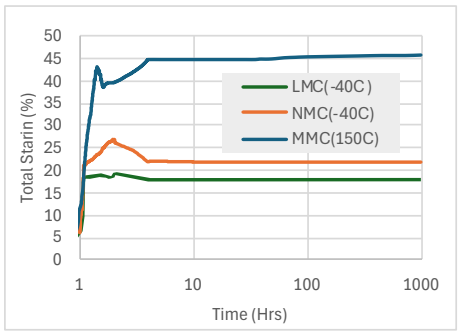

Figure 23. Total Strain.

3.1.4 With Stress Relaxation and Mullin's effect under Thermal Cycling (3D Quarter Symmetry Results)

For both the thermal cycling cases, contact Pressure is below the minimum Contact Pressure criteria of 1 MPa at corners & other areas of contact interfaces at the end of the three cycles due to Cooling and combination of Stress Relaxation & Mullin's Effect (Figure 24.b. and Figure 25.b.). Hence would not be leak proof.

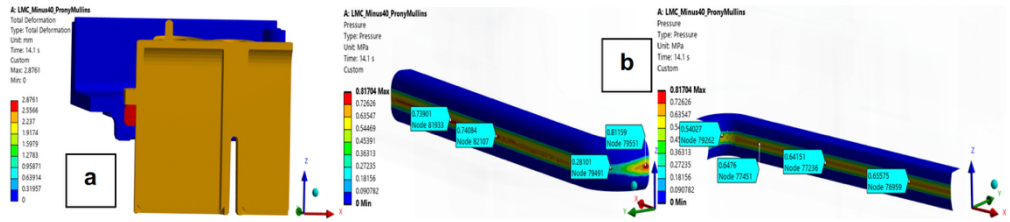

Figure 24. LMC: a. Total Deformation, b. Contact Pressure of Seal.

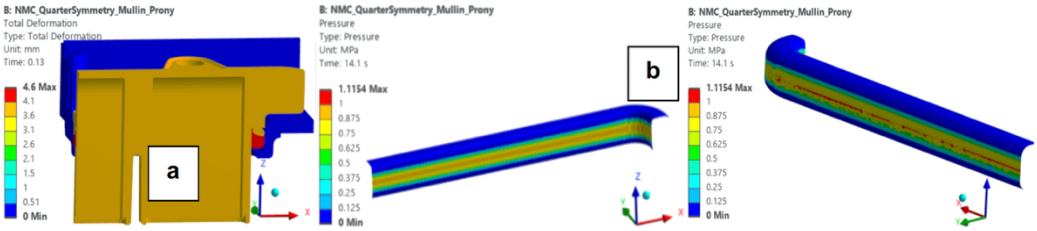

Figure 25. NMC: a. Total Deformation, b. Contact Pressure of Seal.

Table 8. Thermal Cycling.

Cases	Max Deformation (mm)	Max Equivalent Strain (%)	Max Contact Pressure (MPa)
LMC	2.9	19.1	0.81
NMC	4.6	31	1.11

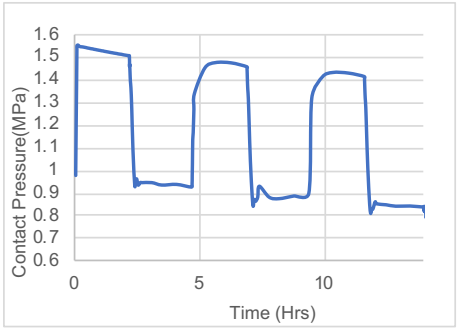

Figure 26. LMC-Contact Pressure.

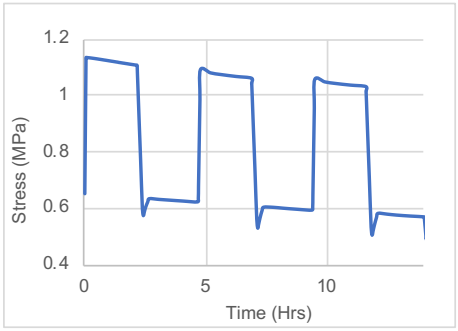

Figure 27. LMC-Stress plot.

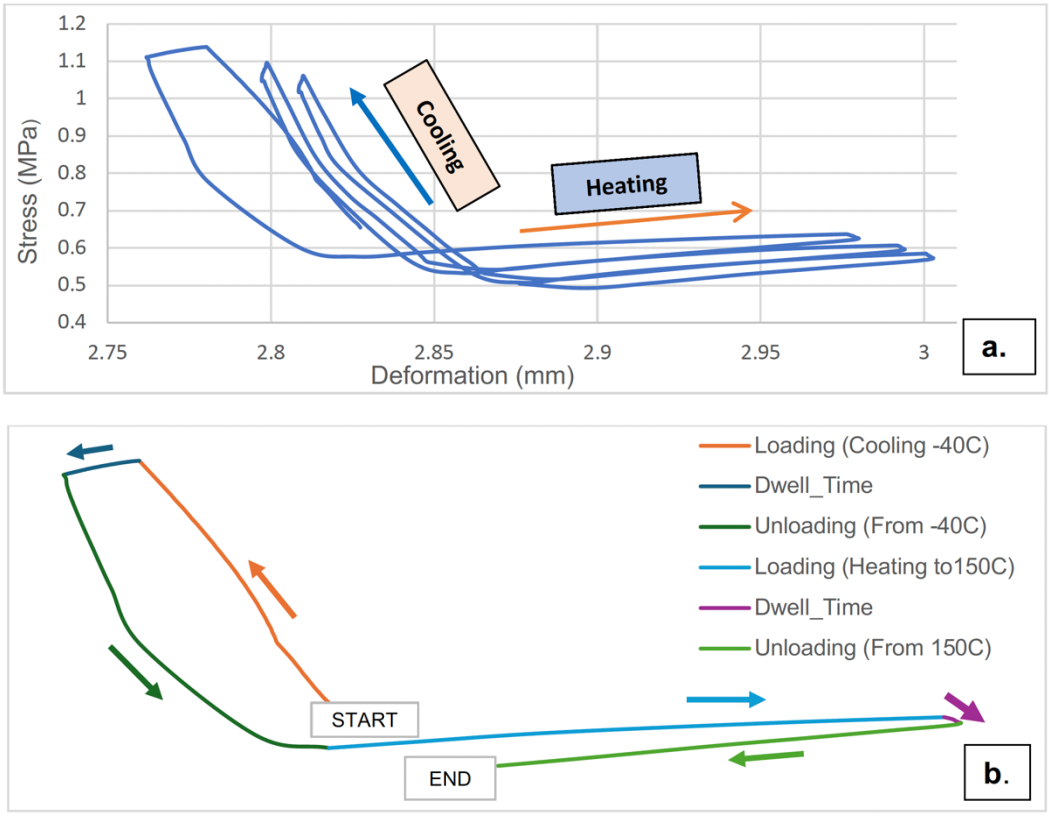

Figure 28. LMC: a. Stress Deformation plot, b. One Cycle Thermal Loading.

Figures 26, 27 and 29 show the Contact Pressure and Stress reduction with number of cycles which is stress softening due to Mullin's Effect. Figure 30 shows the Total Seal Strains has negligible impact with the number of cycles.

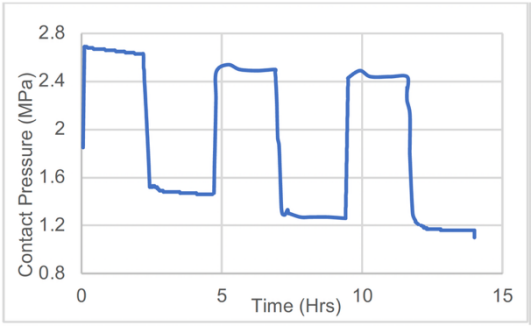

Figure 29. NMC-Contact pressure.

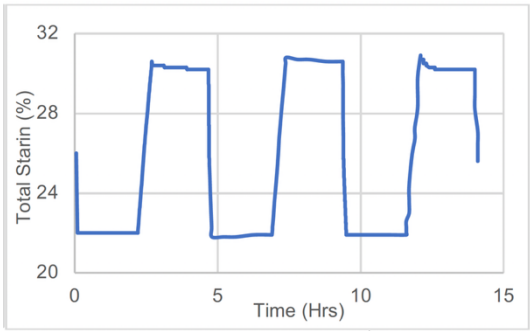

Figure 30. NMC-Strain.

4 Verification and Validation

Figure 30 illustrates a Transparent Housing used to visualize Contact interaction between the EPDM Seal and Aluminium Housing, highlighting insufficient contact zones. The observed Contact Behaviour correlates well with simulation results, providing clear direction for design improvements.

A Quasi-Static solution [10] is employed to address convergence issues in quasi-static analysis. Semi-Implicit method [11] is used as a fallback when the implicit solver fails to converge. This hybrid method is particularly effective for highly nonlinear problems that temporarily resist convergence.

4.1 Assumptions and limitations

Coefficient of Thermal Expansion (CTE) and Friction Coefficient are treated as constants due to lack of temperature-dependent data. Based on seal supplier feedback, this simplification has negligible impact compared to temperature effects on Shear Moduli. Since Shear is the Dominant Failure Mode, the results remain valid for the sealing application under present study. Maximum Contact Pressure values apply to a small contact surface between the components and is not an individual nodal value as the Contact Pressure location varies across Material Conditions & Cross-Section.

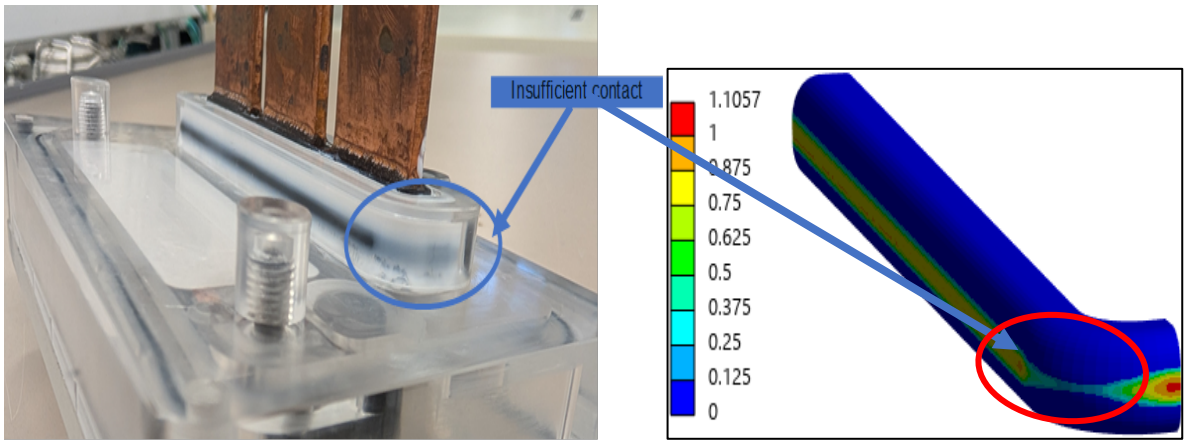

Figure 31. Clear Housing (shows area with Insufficient Contact).

5 Conclusions

This investigation was focused on the evaluation of EPDM PIP seals to improve the durability and performance & has compared the effects of temperature, time and material conditions on the seal force, seal deformation, seal strains and contact pressure with dissimilar CTE's of materials. Though, Stress Relaxation & Mullins Effect has negligible impact in seal deformation and seal strains but has a significant impact on the contact pressure. These kinds of studies will be helpful in checking the seal leakage and integrity at extremely high and low temperatures. Also, we can understand how the seal joint behaves with time and retains minimum contact pressure in all material conditions.

- 2D Plane Strain: This approach gives an idea of the Seal behaviour at various material and Temperature conditions but is only limited to a particular cross-section and cannot predict the behaviour across varying geometry.
- 3D Quarter Symmetry: This approach shows clear insight on the Seal performance at various Material and Temperature conditions also. Quarter symmetry results are on par with full scale physical test results and is computationally efficient.
- Thermal Aging/Stress Relaxation: Shows significant impact on Contact Pressure during operating life cycle but has negligible effect on Strains and Deformations.
- Mullin's Effect: From thermal cycling study, it is evident that the stress softening (reduction in stresses with subsequent cycles) occurs due to Mullin's effect. Also contact pressure reduces during Thermal cycling.
- Verification & Validation: In comparison to the Physical Test, the Simulation results correlate very well and gives the design direction for improvement to achieve the desired performance

of EPDM seal used in the present application under various Material and Temperature conditions.

- Future Work: Parametric and Shape optimization of the seal can be performed using MDO (Multidisciplinary optimization) method to obtain optimal seal designs which meet all the requirements.

6 Acknowledgement

Bednarz Jack A, Global Chief Engineer, Mechanical, PDS - eHW Execution, BorgWarner, US
Ravi Kumar, Senior Hardware Design Manager, PDS - eHW Execution, BorgWarner, India
Abhijit Kaisare, Mechanical Engineering Manager, PDS - eHW Execution, BorgWarner, India
Sridhar G, Mechanical Staff Engineer, PDS - eHW Execution, BorgWarner, India.

7 Nomenclature

LMC	Least Material Condition
NMC	Nominal Material Condition
MMC	Maximum Material Condition
PIP	Press-in-place
CTE	Coefficient of Thermal Expansion
EPDM	Ethylene Propylene Diene Monomer

8 References

[1] Ferry, J.D. (1980). Viscoelastic properties of polymers. 3rd edition: John Wiley & Sons.

[2] Johan Sandström, " Simulation and calibration of rubber materials for seals", The Finnish Research Programme on Nuclear Power Plant Safety 2015, 2018, pp. 1-17.

[3] P. K. Freakley och A. Payne, Theory and Practice of Engineering with Rubber, Applied Science Publishers, 1978.

[4] J. H. Sällström, J. Sandström och S.-E. Sällberg," Täthet hos flänsförband mellan stora polyetenrör och ventiler – experimentell och numerisk studie," Svenskt Vatten Utveckling, Bromma, 2016.

[5] Xu Q, Engquist B., 2018, "A mathematical model for fitting and predicting relaxation modulus and simulating viscoelastic responses", Proc. R. Soc. A 474: 20170540.

[6] Yijie Liu, "A review of the effect of temperature on the performance of viscoelastic dampers", Journal of Physics: Conference Series 2798, 2024, pp 2-8.

[7] Zhanbin Wang, "Research on fatigue failure mode and failure theory of rubber", ICETMS 2021, Journal of Physics: Conference Series 2076 (2021), pp 2-10.

[8] William W Feng, John O Hallquist, "Mullins Effect in Rubber part Two: Biaxial", 14th International LS_DYNA User Conference, 2016, pp 1-11.

[9] ANSYS Inc., Mullins Effect Theory. ANSYS Documentation.

[10] ANSYS Inc., Solver Controls – Quasi-Static Analysis. ANSYS Workbench Simulation.

[11] ANSYS Inc., Semi-Implicit Method in Advanced Analysis. ANSYS Advanced Solver Documentation.

[12] Dorfmann A, Muhr A ed. (Rotterdam: A.A. Balkema). (1999). Constitutive Models for Rubber.